Attenuation of cardiac remodeling after myocardial infarction by muscle LIM protein-calcineurin signaling at the sarcomeric Z-disc

Joerg Heineke*†, Hartmut Ruetten‡, Christian Willenbockel*, Sandra C. Gross*, Marian Naguib*, Arnd Schaefer*, Tibor Kempf*, Denise Hilfiker-Kleiner*, Pico Caroni§, Theresia Kraft¶, Robert A. Kaiser†, Jeffery D. Molkentin†, Helmut Drexler*, and Kai C. Wollert*‖

Departments of *Cardiology and Angiology, and ¶Molecular and Cellular Physiology, Hanover Medical School, 30625 Hanover, Germany; ‡Aventis Pharma, 65926 Frankfurt, Germany; §Friedrich-Miescher Institute, 4058 Basel, Switzerland; and †Department of Molecular Cardiovascular Biology, Children's Hospital Medical Center, Cincinnati, OH 45229-3039

Edited by Louis J. Ignarro, University of California School of Medicine, Los Angeles, CA, and approved December 15, 2004 (received for review July 28, 2004)

Adverse left ventricular (LV) remodeling after myocardial infarction (MI) is a major cause for heart failure. Molecular modifiers of the remodeling process remain poorly defined. Patients with heart failure after MI have reduced LV expression levels of muscle LIM protein (MLP), a component of the sarcomeric Z-disk that is involved in the integration of stress signals in cardiomyocytes. By using heterozygous MLP mutant ($MLP^{+/-}$) mice, we explored the role of MLP in post-MI remodeling. LV dimensions and function were similar in sham-operated WT and $MLP^{+/-}$ mice. After MI, however, $MLP^{+/-}$ mice displayed more pronounced LV dilatation and systolic dysfunction and decreased survival compared with WT mice, indicating that reduced MLP levels predispose to adverse LV remodeling. LV dilatation in $MLP^{+/-}$ mice was associated with reduced thickening but enhanced elongation of cardiomyocytes. Activation of the stress-responsive, prohypertrophic calcineurin–nuclear factor of activated T-cells (NFAT) signaling pathway was reduced in $MLP^{+/-}$ mice after MI, as shown by a blunted transcriptional activation of NFAT in cardiomyocytes isolated from $MLP^{+/-}$/NFAT-luciferase reporter gene transgenic mice. Calcineurin was colocalized with MLP at the Z-disk in WT mice but was displaced from the Z-disk in $MLP^{+/-}$ mice, indicating that MLP is essential for calcineurin anchorage to the Z-disk. *In vitro* assays in cardiomyocytes with down-regulated MLP confirmed that MLP is required for stress-induced calcineurin–NFAT activation. Our study reveals a link between the stress sensor MLP and the calcineurin–NFAT pathway at the sarcomeric Z-disk in cardiomyocytes and indicates that reduced MLP–calcineurin signaling predisposes to adverse remodeling after MI.

heart failure | stress signaling

Chronic heart failure is a worldwide epidemic. Recently, a fundamental shift in the underlying etiology of heart failure has occurred, in which the most common cause of heart failure is no longer hypertension or valvular disease, but myocardial infarction (MI) (1). MI induces profound alterations of left ventricular (LV) architecture with scar formation, ventricular dilatation, and hypertrophy of the noninfarcted (remote) myocardium (2). Biomechanical stress and humoral growth factors are important mediators of this remodeling process (3, 4). At the level of the single cardiomyocyte, post-MI LV remodeling is characterized by increases in cell diameter and cell length and alterations in gene expression levels (5–7).

The Z-disk is a multiprotein complex located at the interface of the cytoskeleton, the contractile apparatus, and the sarcolemma in cardiomyocytes (8). Muscle LIM protein (MLP), which is tethered to the Z-disk via its interacting partners, α-actinin and telethonin, has been proposed to be an essential part of the mechanical stretch sensor machinery (9) and to be involved in the transmission of humoral growth signals in cardiomyocytes (10). Intriguingly, myocardial MLP levels are reduced by ≈50% in patients with heart failure after MI (11). However, the functional significance of this observation is not clear (12). Moreover, the downstream effector pathways activated by MLP have remained elusive. Interestingly, the Ca^{2+}/calmodulin-dependent phosphatase calcineurin, which has a major impact on cardiomyocyte growth and gene expression by promoting dephosphorylation and nuclear translocation of nuclear factor of activated T cells (NFAT) transcription factors (13), forms a trimeric complex with α-actinin and calsarcin-1 at the Z-disk, suggesting a close proximity between MLP and calcineurin (14).

By using heterozygous MLP mutant ($MLP^{+/-}$) mice, which display no apparent phenotype at baseline, we explored the signaling pathways downstream of MLP and the impact of MLP on post-MI remodeling.

Materials and Methods

Experimental Animals. Generation and PCR genotyping of MLP mutant mice have been described (15). For *in vivo* assessments of NFAT transcriptional activity, $MLP^{+/-}$ mice were crossed with NFAT-luciferase reporter gene transgenic (NFAT-Luc-tg) mice (16). MI was induced during propofol (10 mg/kg, i.v.) and enflurane (4%) anesthesia by permanent coronary artery ligation in 8- to 12-week-old WT ($MLP^{+/+}$), $MLP^{+/-}$, $MLP^{+/+}$/NFAT-Luc-tg, and $MLP^{+/-}$/NFAT-Luc-tg mice. Control mice underwent a sham operation. Unless otherwise stated, mice were analyzed 6 weeks after surgery. All animal procedures were approved by government authorities.

Echocardiography and Left Heart Catheterization. Transthoracic echocardiography was performed with a linear 15-MHz transducer (ATL HDI 5000 CV, Bothell, WA) (17). Short-axis 2D images and M-mode tracings were recorded and analyzed by a sample-blinded investigator (A.S.) at the papillary muscle level in mice sedated with ketamine (50 mg/kg, i.p.) and xylazine (5 mg/kg, i.p.). LV ejection fraction was calculated as [(LVEDA − LVESA)/LVEDA] × 100, where LVEDA and LVESA denote LV end-diastolic and end-systolic areas, respectively (18). LV hemodynamics were recorded and analyzed by a sample-blinded investigator (H.R.) by using a 1.4 F micromanometer conductance catheter (SPR-7129, Millar Instruments, Houston) inserted via the right carotid artery during enflurane (4%) anesthesia (19). Steady-state LV pressure and conductance data were

This paper was submitted directly (Track II) to the PNAS office.

Abbreviations: Akt, protein kinase B; BNP, B-type natriuretic peptide; ERK, extracellular signal-regulated kinase; LV, left ventricular; MCIP1, exon 4 variant of modulatory calcineurin-interacting protein-1; MHC, myosin heavy chain; MI, myocardial infarction; MLP, muscle LIM protein; $MLP^{+/-}$, heterozygous MLP mutant; NFAT, nuclear factor of activated T cells; NFAT-Luc-tg, NFAT-luciferase reporter gene transgenic.

‖To whom correspondence should be addressed. E-mail: wollert.kai@mh-hannover.de.

sampled at a rate of 1 kHz. LV ejection fraction was calculated as [(LVEDV − LVESV)/LVEDV] × 100, where LVEDV and LVESV denote LV end-diastolic and end-systolic volumes, respectively.

Histological Analysis. Left ventricles were cut into three transverse slices; the apical and basal slices were snap-frozen in liquid N_2 and stored at −80°C for later isolation of RNA and protein. Cryosections were prepared from the middle slice. Myocardial infarct sizes were determined by planimetry in three cryosections stained with hematoxylin/eosin and expressed as [%] of LV circumference (20).

Immunostaining. Expression patterns of MLP, calcineurin, calsarcin-1, and α-actinin were determined by immunostaining and confocal laser scanning microscopy. Generation of the polyclonal antibody against rat MLP has been described (21). mAbs against the calcineurin A-subunit and calsarcin-1 were obtained from BD Transduction Laboratories, San Diego. A mAb directed against α-actinin and FITC- or tetramethylrhodamine B isothiocyanate-coupled secondary antibodies were purchased from Sigma.

Cardiomyocyte Isolation. LV cardiomyocytes were isolated by collagenase digestion 3 weeks (for luciferase measurements) or 6 weeks (for morphometry) after sham operation or MI (22). Luciferase activities were determined as described (16). For morphometric measurements, myocytes were suspended in 30 mM KCl for relaxation and subsequently fixed in 2% glutaraldehyde. Cell length and width were determined by phase-contrast microscopy and a digital image analyzer (23).

RNA Dot Blot Analysis. Total RNA was extracted from the remote LV by the TRIzol reagent (Invitrogen). Expression levels of atrial natriuretic peptide, B-type natriuretic peptide (BNP), skeletal α-actin, α-myosin heavy chain (α-MHC), β-MHC, sarco(endo)plasmic reticulum Ca^{2+} ATPase-2, phospholamban, the exon 4 variant of modulatory calcineurin-interacting protein-1 (MCIP1), and β-actin were determined by mRNA dot-blot analysis using ^{32}P-labeled cDNA probes (available on request).

Immunoblotting. Protein expression levels were determined by immunoblotting using antibodies directed against extracellular signal-regulated kinases 1 and 2 (ERK1 and ERK2), phospho-ERK1/ERK2 (Thr-202/Tyr-204), protein kinase B (Akt1), Ser-473-phospho-Akt1, glycogen synthase kinase (GSK)-3β, and Ser-9-phospho-GSK3β from Cell Signaling Technology (Beverly, MA), antibodies directed against calcineurin A and calsarcin-1 from BD Transduction Laboratories, and the polyclonal anti-MLP antibody.

Immunoprecipitation. Calcineurin-A was immunoprecipitated from LV tissue lysates by using a polyclonal anti-calcineurin A antibody from Chemicon and protein A agarose (Invitrogen). Precipitates were washed with PBS, boiled, subjected to SDS/PAGE, and transferred to nitrocellulose membranes. Membranes were immunoblotted with the polyclonal anti-MLP antibody.

Cardiomyocyte Culture. Ventricular cardiomyocytes were isolated from 1- to 3-day-old Sprague–Dawley rats as described (23). Cells were plated overnight in gelatin-coated culture dishes (Nunc) or silicone elastomer plates (Bioflex, Flexcell International, McKeesport, PA) in DMEM/medium 199 (4:1), supplemented with 10% horse serum, 5% FCS, glutamine, and antibiotics. The next morning, myocytes were switched to DMEM/medium 199 supplemented only with glutamine and antibiotics.

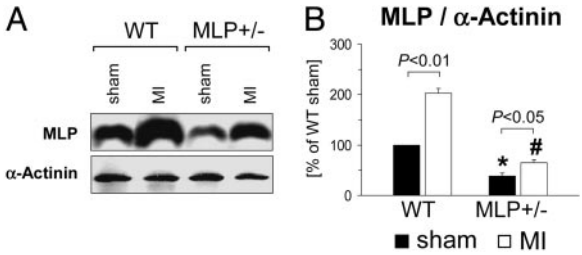

Fig. 1. Reduced myocardial MLP expression levels in $MLP^{+/-}$ mice. LV myocardial MLP and α-actinin protein expression levels were determined by immunoblotting 6 weeks after sham operation or MI. (*A*) Typical blots are shown. (*B*) Data from $n = 4$–5 mice per group are summarized. *, $P < 0.05$ vs. sham-operated WT mice; #, $P < 0.01$ vs. infarcted WT mice.

Transfection with Plasmid Vectors and Antisense Oligonucleotides. A calcium phosphate procedure was used to transfect cardiomyocytes with p3xNFAT-GL, a luciferase reporter plasmid driven by three NFAT-binding sites (24). Cardiomyocytes were cotransfected with an antisense oligonucleotide (AS4) directed against the ATG translation start site of rat MLP mRNA to specifically down-regulate MLP protein expression levels. Transfection of cardiomyocytes with AS4 (0.5 μM) down-regulates MLP protein expression by ≈50% (10). A corresponding scrambled oligonucleotide, which does not suppress MLP expression levels (10), served as a negative control. Twenty-four hours after transfection, cells were stimulated with endothelin-1 (Sigma) or subjected to continuous cycles of stretch and relaxation (0.5 Hz, 15% radial stretch) by using the Flexercell Strain Unit FX-3000 (Flexcell). Luciferase activities were measured by using a Lumat LB 9501 luminometer (Berthold, Nashua, NH) (24).

Statistical Analysis. Data are presented as mean ± SEM. Differences between groups were analyzed by one-way ANOVA followed by Student-Newman-Keuls post hoc test. Post-MI survival was analyzed by the log-rank test. A two-tailed P value < 0.05 was considered to indicate statistical significance.

Results

Reduced Myocardial MLP Expression Levels in $MLP^{+/-}$ Mice. First, we established that $MLP^{+/-}$ mice can be used to study post-MI remodeling in the context of low MLP expression levels (Fig. 1). After a sham operation, $MLP^{+/-}$ mice had 61 ± 7% lower MLP protein levels as compared with WT mice. MLP levels increased in the remote LV both in WT and $MLP^{+/-}$ mice after MI (2.0 ± 0.1-fold and 1.7 ± 0.2-fold, respectively). MLP expression levels in the remote LV were 68 ± 8% lower in $MLP^{+/-}$ as compared with WT mice. In contrast to MLP, expression levels of the Z-disk protein α-actinin were not induced after MI and did not differ between WT and $MLP^{+/-}$ mice (Fig. 1 and data not shown).

Adverse LV Remodeling and Increased Mortality in $MLP^{+/-}$ Mice After MI. Functional adaptation after MI was determined by echocardiography (Fig. 2 *A* and *B*) and LV pressure-conductance catheterization (Fig. 2 *C* and *D*). After a sham operation, LV diameters and systolic or diastolic functional indices were not significantly different between WT and $MLP^{+/-}$ mice (Fig. 2 *A–D*). Mean infarct sizes were comparable in WT and $MLP^{+/-}$ mice undergoing echocardiography (31 ± 3% vs. 33 ± 3%) and LV catheterization (33 ± 3% vs. 30 ± 2%). With these moderate infarct sizes, WT mice developed some degree of LV dilatation but did not show signs of LV failure [no significant increases in LV end-diastolic pressure, right ventricular weights, or lung weights (Fig. 2*D* and data not shown)]. $MLP^{+/-}$ mice developed more pronounced LV dilatation and had a significantly worse LV

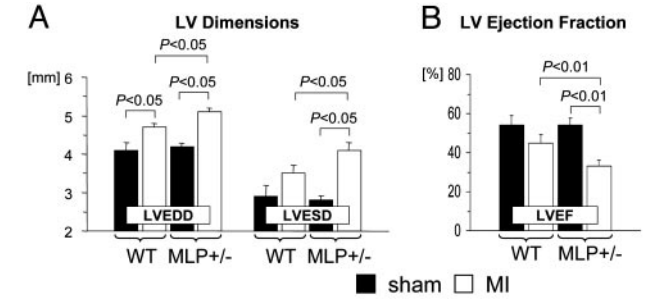

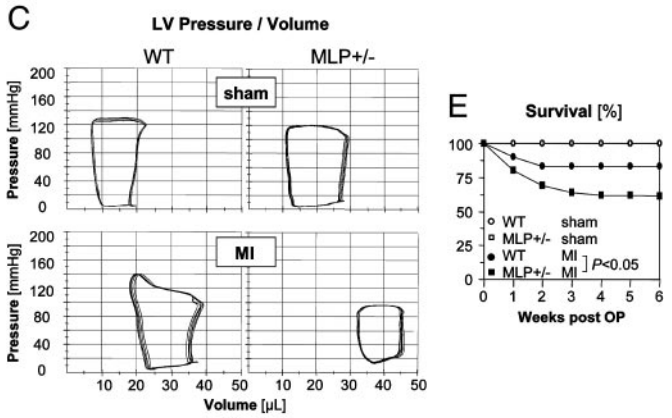

D

		WT		MLP+/-	
		sham	MI	sham	MI
		(n=4)	(n=12)	(n=4)	(n=16)
LVEDV	[µl]	29±6	37±4	33±3	45±2
LVESV	[µl]	12±3	22±4	11±1	32±3*,#
LVEF	[%]	62±3	49±4	69±4	36±4*,#
LVEDP	[mmHg]	7±1	10±1	6±2	11±2
LVESP	[mmHg]	140±10	128±9	129±8	114±8
CO	[µl/min]	9838±1624	8262±695	10531±1380	6815±741
dP/dt_{max}	[mmHg/s]	12736±1165	8533±656	11860±432	7794±664
dP/dt_{min}	[mmHg/s]	-10399±473	-6778±566	-9428±653	-6179±480
τ	[ms]	7.2±0.4	9.4±0.4	7.1±0.5	9.6±0.5
HR	[min^{-1}]	490±12	462±10	442±30	469±8
LV/BW	[mg/g]	3.9±0.3	4.1±0.1	3.7±0.1	4.2±0.2
RV/BW	[mg/g]	0.7±0.1	0.8±0.1	0.7±0.1	0.9±0.1
BW	[g]	32±2	33±1	33±2	33±1

Fig. 2. Enhanced LV dilatation, reduced systolic function, and increased mortality after MI in $MLP^{+/-}$ mice. (*A* and *B*) Echocardiography was performed 6 weeks after sham operation (filled bars) or MI (empty bars). Data are from $n = 7$ sham-operated mice per genotype, $n = 18$ infarcted WT mice, and $n = 30$ infarcted $MLP^{+/-}$ mice. LVEDD and LVESD denote LV end-diastolic and end-systolic diameters, respectively; LVEF, LV ejection fraction. (*C* and *D*) Pressure-volume loops were recorded 6 weeks after sham operation or MI. (*C*) Representative recordings are shown. (*D*) Data are summarized. LVEDV and LVESV denote LV end-diastolic and end-systolic volumes, respectively; LVEF, LV ejection fraction; LVEDP and LVESP, LV end-systolic and end-diastolic pressures, respectively; CO, cardiac output; dP/dt_{max}, maximal rate of pressure development; dP/dt_{min}, maximal rate of pressure decay; τ, monoexponential time constant of LV relaxation; HR, heart rate; LV, LV weight; RV, right ventricular weight; BW, body weight. *, $P < 0.05$ vs. sham-operated $MLP^{+/-}$ mice; #, $P < 0.05$ vs. infarcted WT mice. (*E*) Six-week mortality rates were assessed in 30 WT and 61 $MLP^{+/-}$ mice surviving for at least 48 h after coronary ligation. Sham-operated WT ($n = 8$) and $MLP^{+/-}$ mice ($n = 7$) served as controls (survival curves in sham-operated mice are superimposed).

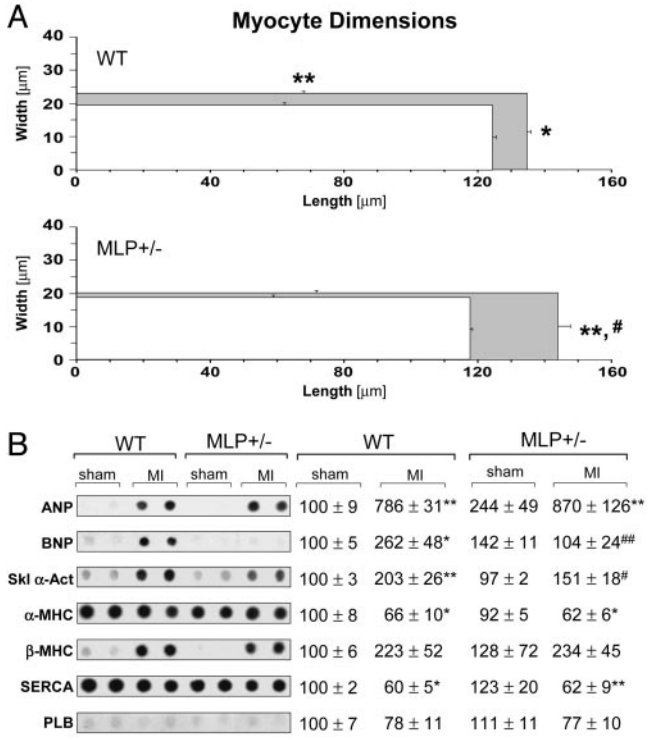

Fig. 3. Cardiomyocyte morphology and gene expression after MI. (*A*) Cardiomyocyte dimensions were determined 6 weeks after sham operation (white rectangles) or MI (gray rectangles). Approximately 100 myocytes per heart were analyzed in $n = 4$–5 mice per group. (*B*) Gene expression levels were determined by mRNA dot blot. Data were normalized to β-actin expression and expressed as [%] of sham-operated WT. (*Left*) Representative blots are shown (two animals per group). (*Right*) Data from $n = 4$–5 sham-operated mice and $n = 7$–11 infarcted mice per group are presented. *, $P < 0.05$; **, $P < 0.01$ vs. sham-operated mice of same genotype; #, $P < 0.05$; ##, $P < 0.01$ vs. infarcted WT mice. ANP, atrial natriuretic peptide; SERCA, sarco(endo)plasmic reticulum Ca^{2+} ATPase-2; PLB, phospholamban.

ejection fraction after MI as compared with WT mice (Fig. 2 *A–D*). LV and right ventricular to body weight ratios were not significantly different between WT and $MLP^{+/-}$ mice after a sham operation or after MI (Fig. 2*D*). The 6-week mortality rate after MI was significantly increased in $MLP^{+/-}$ mice as compared with WT mice (Fig. 2*E*); no sham-operated WT or $MLP^{+/-}$ mouse died during the same observation period.

Cardiomyocyte Morphology and Gene Expression After MI. To explore the cellular basis for adverse post-MI remodeling in $MLP^{+/-}$ mice, LV cardiomyocytes were isolated from WT and $MLP^{+/-}$ mice and analyzed by single-cell morphometry. After a sham operation, mean cardiomyocyte diameter and length were not significantly different between WT and $MLP^{+/-}$ mice (Fig. 3*A*). After MI in WT mice, myocytes in the remote LV developed significant increases in cell diameter and length (Fig. 3*A*). Cardiomyocyte hypertrophy in WT mice was associated with marked alterations in gene expression levels (up-regulation of atrial natriuretic peptide, BNP, and skeletal α-actin; down-regulation of α-MHC and sarco(endo)plasmic reticulum Ca^{2+} ATPase-2) (Fig. 3*B*). Myocytes isolated from the remote LV of $MLP^{+/-}$ mice displayed a distinct hypertrophic response with more pronounced cell elongation but no significant increases in cell diameter (Fig. 3*A*); there was no significant induction of BNP and skeletal α-actin after MI in $MLP^{+/-}$ mice (Fig. 3*B*). These data indicate that certain features of the hypertrophic response after MI (i.e., transverse cardiomyocyte growth, induc-

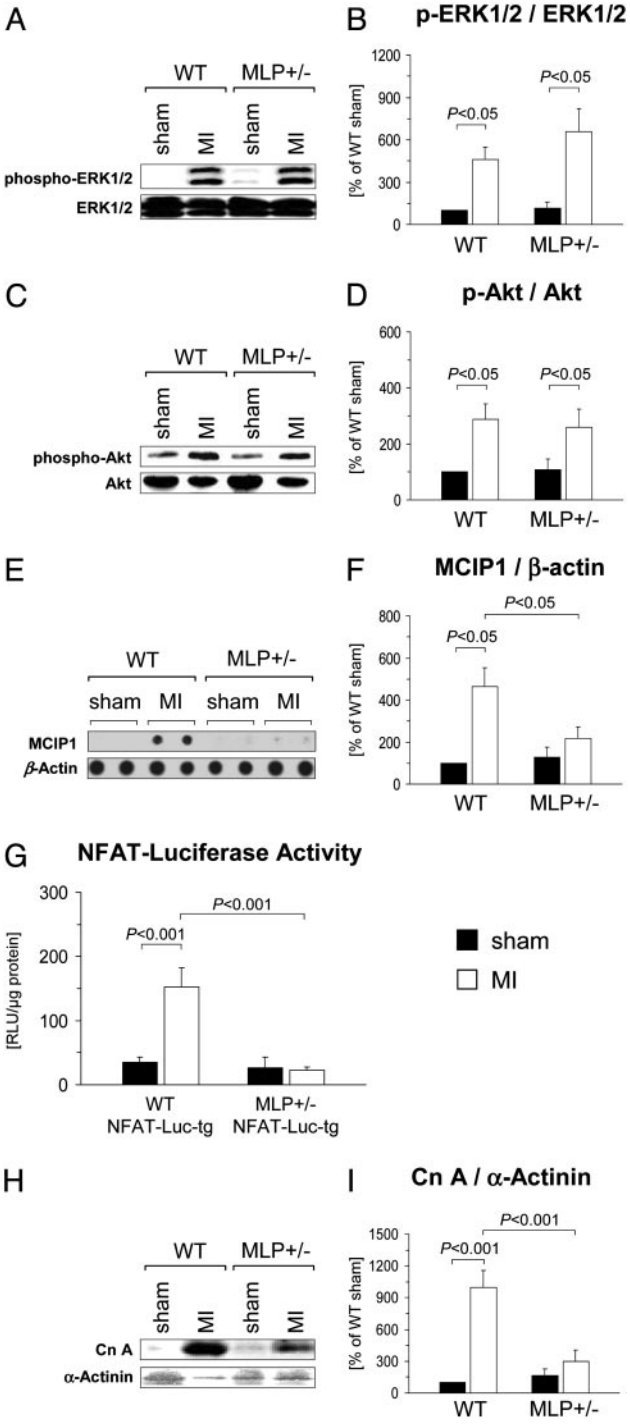

Fig. 4. Signaling pathway activation in WT and MLP$^{+/-}$ mice after MI. (*A–D*) LV myocardial expression levels of ERK1/2, phospho-ERK1/2, Akt1, and phospho-Akt were determined by immunoblotting 6 weeks after sham operation or MI. (*A* and *C*) Typical blots are shown. (*B* and *D*) Data from $n = 3–5$ sham-operated mice (filled bars) and $n = 9–10$ infarcted mice (empty bars) per group are presented. (*E* and *F*) Expression of the exon 4 variant of MCIP1 was determined by mRNA dot-blot analysis and normalized to β-actin expression. (*E*) Typical blots from two animals per group are shown. (*F*) Data from $n = 3–6$ sham-operated mice (filled bars) and $n = 7–11$ infarcted mice (empty bars) are summarized. (*G*) NFAT-luciferase reporter activity was measured in cardiomyocytes isolated from MLP$^{+/+}$ (WT)/NFAT-Luc-tg and MLP$^{+/-}$/NFAT-Luc-tg mice 3 weeks after MI (empty bars) or sham (filled bars) operation. Data from three to five animals per group are shown. (*H* and *I*) Calcineurin A and α-actinin protein expression levels were analyzed by immunoblotting. (*H*) Typical blots are shown. (*I*) Data from $n = 6–7$ animals per group (filled bars, sham; empty bars, MI) are summarized.

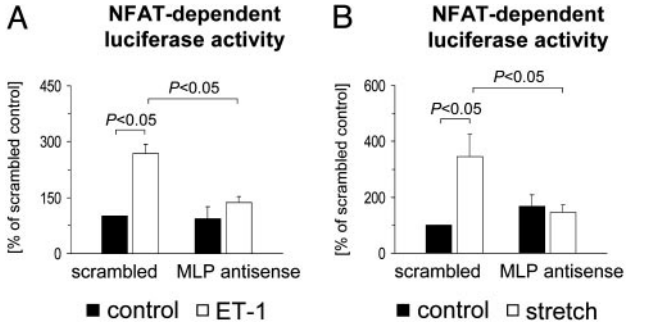

Fig. 5. MLP is required for NFAT activation in cardiomyocytes. Cultured cardiomyocytes were transfected with an MLP antisense oligonucleotide or a scrambled control oligonucleotide (0.5 µM each). All cells were cotransfected with a luciferase reporter plasmid driven by three NFAT consensus binding sites. Cells were then stimulated for 24 h with 25 nM endothelin-1 (*A*) or subjected to 24 h of cyclic stretch (*B*). Data from $n = 4–6$ experiments are presented.

tion of specific embryonic genes) critically depend on sufficient MLP expression levels.

Impaired Calcineurin–NFAT Signaling After MI in MLP$^{+/-}$ Mice. To characterize the effector pathways downstream from MLP, we determined the phosphorylation status of ERK1/2 and Akt1, both of which have been implicated in stress-induced cardiomyocyte growth and gene expression (25). Phosphorylation (activation) of ERK1/2 and Akt1 was similarly enhanced in the remote LV in WT and MLP$^{+/-}$ mice (Fig. 4 *A-D*). To assess the activation level of the calcineurin–NFAT pathway, we determined the mRNA abundance of the exon 4 variant of the muscle cell-enriched gene MCIP1, which is controlled by an intragenic cluster of NFAT consensus binding sites (26). MCIP1 expression levels were significantly increased in the remote LV in WT mice; by contrast, there was no significant induction of MCIP1 after MI in MLP$^{+/-}$ mice (Fig. 4 *E* and *F*). To obtain a more direct assessment of NFAT transcriptional activity, MLP$^{+/-}$ mice were crossed with NFAT-Luc-tg mice. NFAT-luciferase activities were not significantly different in cardiomyocytes isolated from sham-operated MLP$^{+/+}$/NFAT-Luc-tg and MLP$^{+/-}$/NFAT-Luc-tg mice (Fig. 4*G*). After MI, NFAT-luciferase activity markedly increased in MLP$^{+/+}$/NFAT-Luc-tg mice but not in MLP$^{+/-}$/NFAT-Luc-tg mice (Fig. 4*G*). LV calcineurin A protein expression levels were not significantly different in sham-operated WT and MLP$^{+/-}$ mice (Fig. 4 *H* and *I*). After MI, calcineurin A expression increased in the remote LV in WT but not significantly in MLP$^{+/-}$ mice (Fig. 4 *H* and *I*).

MLP Is Required for Endothelin-1 and Stretch-Induced NFAT Activation in Cardiomyocytes. Reduced expression levels of MCIP1 and reduced NFAT-luciferase reporter gene induction in MLP$^{+/-}$ mice after MI suggested that sufficient MLP levels are required for calcineurin–NFAT activation. To further test this concept, MLP protein expression was down-regulated by ≈50% in cultured cardiomyocytes by a specific antisense oligonucleotide (AS4) (10). Transfection with AS4 prevented the increases in NFAT transcriptional activity induced by endothelin-1 or mechanical stretch (Fig. 5), indicating that calcineurin–NFAT activation in response to external stress depends on MLP.

MLP Is Required for Calcineurin Localization to the Z-Disk. Coimmunostaining of LV tissue sections from WT mice with anti-MLP and anti-calcineurin antibodies followed by confocal laser microscopy confirmed previous reports (14, 27) that MLP and calcineurin are colocalized at the cardiac Z-disk (Fig. 6*A*). Notably, MLP and calcineurin could be coimmunoprecipitated

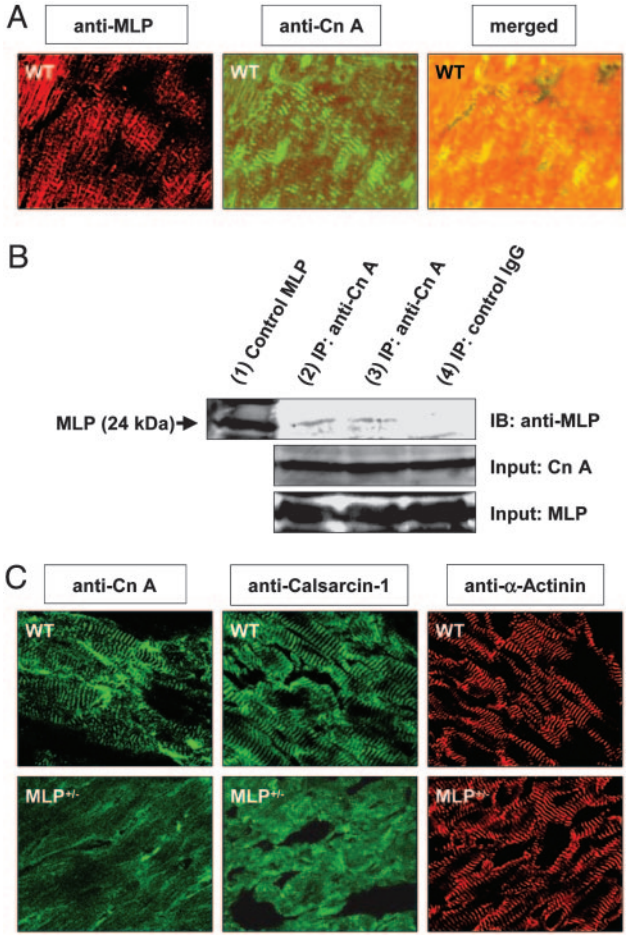

Fig. 6. MLP is required for calcineurin anchorage to the sarcomeric Z-disk. (*A*) A LV cryosection obtained from a WT mouse was coimmunostained against MLP (*Left*) and calcineurin A (Cn A, *Center*) and analyzed by confocal laser microscopy. (*Right*) The merged image indicates colocalization of MLP and calcineurin. (*B*) Immunoprecipitation (IP) of MLP by the anti-calcineurin A antibody (lanes 2 and 3), but not IgG control antibody (lane 4), from WT LV tissue lysates reveals a physical interaction of MLP and calcineurin. A MLP standard was loaded in lane 1. The calcineurin A and MLP IP inputs are shown; IB denotes immunoblotting. (*C*) Adjacent LV tissue sections from WT and $MLP^{+/-}$ mice were immunostained against calcineurin A, calsarcin-1, and α-actinin and analyzed by confocal laser microscopy. The striated staining pattern of calcineurin A and calsarcin-1 observed in WT mice is lost in $MLP^{+/-}$ mice. By contrast, anti-α-actinin staining reveals prominent striations in WT and $MLP^{+/-}$ mice.

from LV tissue lysates of WT mice (Fig. 6*B*), implying that MLP and calcineurin interact, either directly or via linker protein(s). To test whether MLP is required for calcineurin anchorage to the Z-disk, calcineurin localization was assessed in WT and $MLP^{+/-}$ mice. Intriguingly, the striated expression pattern of calcineurin in WT mice was lost in $MLP^{+/-}$ mice (Fig. 6*C*). Calcineurin dropout from the Z-disk was observed in nonoperated (Fig. 6*C*) and infarcted (data not shown) $MLP^{+/-}$ mice. Because calsarcin-1 is a binding partner of calcineurin at the Z-disk, we also analyzed calsarcin-1 localization in WT and $MLP^{+/-}$ hearts. Much like calcineurin, calsarcin-1 was largely dislocated from the Z-disk in $MLP^{+/-}$ mice (Fig. 6*C*). Immunostaining of adjacent cryosections with an anti-α-actinin antibody revealed prominent striations in WT and $MLP^{+/-}$ mice, thereby excluding gross Z-disk abnormalities in $MLP^{+/-}$ mice (Fig. 6*C*). No staining was detected when the primary anti-MLP, anti-calcineurin, anti-calsarcin-1, or anti-α-actinin antibodies were omitted (data not shown).

Discussion

The sarcomeric Z-disk functions as a physical anchor for myofilament and cytoskeletal proteins and a pivot for reception and transduction of mechanical and biochemical stress signals (8). Mutations in Z-disk proteins that may affect both the structural integrity of the Z-disk and/or the transmission of intracellular signals may cause dilated cardiomyopathy in mice and patients (15, 28, 29). Although it has been reported that myocardial MLP levels are reduced by $\approx$50% in patients with heart failure after MI (11), the role of MLP in post-MI cardiac remodeling has remained uncertain. Using $MLP^{+/-}$ mice, the present study demonstrates that sufficient expression levels of MLP are critically required to limit adverse cardiac remodeling (LV dilatation and systolic dysfunction) and improve survival after MI.

At the level of the single cardiomyocyte, adverse post-MI remodeling in $MLP^{+/-}$ mice was associated with a distinct hypertrophic response, characterized by pronounced cell elongation and lack of significant cell thickening. The striking differences in cardiomyocyte shape between WT and $MLP^{+/-}$ mice after MI may represent the cellular basis of enhanced LV dilatation in $MLP^{+/-}$ mice, because inadequate cardiomyocyte thickening in combination with disproportionate cell lengthening has been associated with LV dilatation after MI (5, 6). Although MLP has been proposed to act as a mechanical stress sensor in cardiomyocytes, the downstream signaling cascades activated by MLP have not been elucidated (8, 9). Several lines of evidence presented in this study indicate that MLP is coupled to the prohypertrophic calcineurin–NFAT pathway in cardiomyocytes. Blunted induction of calcineurin A protein expression in $MLP^{+/-}$ mice after MI provided a first clue in this regard, because activated calcineurin has been shown to reinforce its own expression (30, 31). The observations that the calcineurin–NFAT-regulated gene MCIP1 is not induced and that an NFAT-luciferase reporter gene is not activated in the remote LV in $MLP^{+/-}$ mice provided strong support for the conclusion that MLP is linked to the calcineurin–NFAT signaling pathway. Along this line, antisense down-regulation of MLP in cultured cardiomyocytes prevented the transcriptional activation of NFAT by mechanical and biochemical stimulation. ERK1/2, Akt, glycogen synthase kinase-3β, and ERK5 (data not shown) were activated to a similar extent in WT and $MLP^{+/-}$ mice after MI, which argues against a critical role of MLP in the activation of these stress-signaling mediators.

Consistent with previous reports (14, 27), calcineurin and MLP were coexpressed at the Z-disk in WT mice in our study. In fact, MLP and calcineurin could be coimmunoprecipitated from LV myocardial lysates, suggesting that MLP and calcineurin interact, either directly or via linker protein(s). Compartmentalization of calcineurin at the Z-disk is essential for coordinated dephosphorylation of NFAT transcription factors, which also are localized at the Z-disk (13, 32). Strikingly, calcineurin was dislocated from the Z-disk in $MLP^{+/-}$ mice (and in MLP antisense oligonucleotide-transfected isolated cardiomyocytes, data not shown), indicating that sufficient MLP levels are required for calcineurin anchorage to the Z-disk. Interestingly, the calcineurin-interacting protein calsarcin-1 (14) also dislocated from the Z-disk in $MLP^{+/-}$ mice, suggesting that MLP is required for stabilization of the calcineurin–calsarcin-1 complex. Although the exact molecular nature of this complex remains to be determined, interaction of MLP and calcineurin at the sarcomeric Z-disk provides a molecular basis for the link between MLP and the calcineurin–NFAT pathway.

Transgenic overexpression of calcineurin in mice promotes increases in cardiomyocyte diameter that culminate in concentric ventricular hypertrophy (33). Conversely, mice carrying a homozygous deletion of calcineurin display a defect in transverse myocyte growth when exposed to hemodynamic load (34). These

observations are consistent with our data that impaired MLP–calcineurin–NFAT signaling is associated with defects in transverse myocyte growth after MI. Along this line, BNP and α-skeletal actin, two genes known to be regulated by calcineurin–NFAT *in vivo* (33, 34), were induced in WT but not in MLP$^{+/-}$ mice after MI. Recent studies using pharmacological (cyclosporin A) or transgenic (MCIP1 overexpression) approaches to inhibit calcineurin activity in cardiomyocytes have arrived at divergent conclusions by suggesting that calcineurin may inhibit (35) or promote (36) adverse cardiac remodeling after MI. Interpretation of these studies is problematic, however, because cyclosporin A mediates calcineurin-independent effects, and MCIP has dual effects on calcineurin activity (37–39). In a recent study (40), the F-box adapter protein atrogin-1 was identified as a unique binding partner of calcineurin and α-actinin at the Z-disk. In the face of hemodynamic stress, atrogin-1 promotes ubiquitin-dependent degradation of calcineurin, resulting in a reduced hypertrophic response (less cardiomyocyte thickening), enhanced cardiac dilation, and enhanced ventricular dysfunction (40). These data are very much reminiscent of our findings that impaired MLP–calcineurin signaling at the Z-disk is associated with blunted transverse myocyte growth, more pronounced ventricular dilation, and contractile dysfunction (i.e., adverse remodeling). Based on these considerations, we propose that the impact of MLP on post-MI ventricular hypertrophy and remodeling is mediated via the calcineurin–NFAT signaling pathway (although we do not discount the possibility that additional MLP-dependent pathways may exist). In the future, enhancement of MLP signaling may provide a new therapeutic strategy to inhibit adverse remodeling after MI.

We thank Mrs. Nelli Otto and Mrs. Susann Busch for expert technical assistance. This work was supported by grants from the Deutsche Forschungsgemeinschaft (Wo 552/2-2) and the Bundesministerium für Bildung und Forschung (Kompetenznetz Herzinsuffizienz) (to K.C.W.) and an early career grant from Hanover Medical School (to J.H.) (HiLF Program).

1. Gheorghiade, M. & Bonow, R. O. (1998) *Circulation* **97,** 282–289.
2. Cohn, J. N., Ferrari, R. & Sharpe, N. (2000) *J. Am. Coll. Cardiol.* **35,** 569–582.
3. Mann, D. L. (1999) *Circulation* **100,** 999–1008.
4. Force, T., Michael, A., Kilter, H. & Haq, S. (2002) *J. Card. Fail.* **8,** S351–S358.
5. Zimmer, H. G., Gerdes, A. M., Lortet, S. & Mall, G. (1990) *J. Mol. Cell. Cardiol.* **22,** 1231–1243.
6. Gerdes, A. M. & Capasso, J. M. (1995) *J. Mol. Cell. Cardiol.* **27,** 849–856.
7. Dorn, G. W., 2nd, Robbins, J. & Sugden, P. H. (2003) *Circ. Res.* **92,** 1171–1175.
8. Pyle, W. G. & Solaro, R. J. (2004) *Circ. Res.* **94,** 296–305.
9. Knoll, R., Hoshijima, M., Hoffman, H. M., Person, V., Lorenzen-Schmidt, I., Bang, M. L., Hayashi, T., Shiga, N., Yasukawa, H., Schaper, W., *et al*. (2002) *Cell* **111,** 943–955.
10. Heineke, J., Kempf, T., Kraft, T., Hilfiker, A., Morawietz, H., Scheubel, R. J., Caroni, P., Lohmann, S. M., Drexler, H. & Wollert, K. C. (2003) *Circulation* **107,** 1424–1432.
11. Zolk, O., Caroni, P. & Bohm, M. (2000) *Circulation* **101,** 2674–2677.
12. Katz, A. M. (2000) *Circulation* **101,** 2672–2673.
13. Vega, R. B., Bassel-Duby, R. & Olson, E. N. (2003) *J. Biol. Chem.* **278,** 36981–36984.
14. Frey, N., Richardson, J. A. & Olson, E. N. (2000) *Proc. Natl. Acad. Sci. USA* **97,** 14632–14637.
15. Arber, S., Hunter, J. J., Ross, J., Jr., Hongo, M., Sansig, G., Borg, J., Perriard, J. C., Chien, K. R. & Caroni, P. (1997) *Cell* **88,** 393–403.
16. Wilkins, B. J., Dai, Y. S., Bueno, O. F., Parsons, S. A., Xu, J., Plank, D. M., Jones, F., Kimball, T. R. & Molkentin, J. D. (2004) *Circ. Res.* **94,** 110–118.
17. Schaefer, A., Klein, G., Brand, B., Lippolt, P., Drexler, H. & Meyer, G. P. (2003) *J. Am. Soc. Echocardiogr.* **16,** 1144–1149.
18. Yang, X. P., Liu, Y. H., Rhaleb, N. E., Kurihara, N., Kim, H. E. & Carretero, O. A. (1999) *Am. J. Physiol.* **277,** H1967–H1974.
19. Badorff, C., Ruetten, H., Mueller, S., Stahmer, M., Gehring, D., Jung, F., Ihling, C., Zeiher, A. M. & Dimmeler, S. (2002) *J. Clin. Invest.* **109,** 373–381.
20. Shiomi, T., Tsutsui, H., Hayashidani, S., Suematsu, N., Ikeuchi, M., Wen, J., Ishibashi, M., Kubota, T., Egashira, K. & Takeshita, A. (2002) *Circulation* **106,** 3126–3132.
21. Arber, S., Halder, G. & Caroni, P. (1994) *Cell* **79,** 221–231.
22. Mitcheson, J. S., Hancox, J. C. & Levi, A. J. (1998) *Cardiovasc. Res.* **39,** 280–300.
23. Wollert, K. C., Taga, T., Saito, M., Narazaki, M., Kishimoto, T., Glembotski, C. C., Vernallis, A. B., Heath, J. K., Pennica, D., Wood, W. I. & Chien, K. R. (1996) *J. Biol. Chem.* **271,** 9535–9545.
24. Fiedler, B., Lohmann, S. M., Smolenski, A., Linnemuller, S., Pieske, B., Schroder, F., Molkentin, J. D., Drexler, H. & Wollert, K. C. (2002) *Proc. Natl. Acad. Sci. USA* **99,** 11363–11368.
25. Sugden, P. H. (2003) *Circ. Res.* **93,** 1179–1192.
26. Yang, J., Rothermel, B., Vega, R. B., Frey, N., McKinsey, T. A., Olson, E. N., Bassel-Duby, R. & Williams, R. S. (2000) *Circ. Res.* **87,** E61–E68.
27. Arber, S. & Caroni, P. (1996) *Genes Dev.* **10,** 289–300.
28. Zhou, Q., Chu, P. H., Huang, C., Cheng, C. F., Martone, M. E., Knoll, G., Shelton, G. D., Evans, S. & Chen, J. (2001) *J. Cell Biol.* **155,** 605–612.
29. Pashmforoush, M., Pomies, P., Peterson, K. L., Kubalak, S., Ross, J., Jr., Hefti, A., Aebi, U., Beckerle, M. C. & Chien, K. R. (2001) *Nat. Med.* **7,** 591–597.
30. Lim, H. W., De Windt, L. J., Steinberg, L., Taigen, T., Witt, S. A., Kimball, T. R. & Molkentin, J. D. (2000) *Circulation* **101,** 2431–2437.
31. Taigen, T., De Windt, L. J., Lim, H. W. & Molkentin, J. D. (2000) *Proc. Natl. Acad. Sci. USA* **97,** 1196–1201.
32. Liu, Y., Cseresnyes, Z., Randall, W. R. & Schneider, M. F. (2001) *J. Cell Biol.* **155,** 27–39.
33. Molkentin, J. D., Lu, J. R., Antos, C. L., Markham, B., Richardson, J., Robbins, J., Grant, S. R. & Olson, E. N. (1998) *Cell* **93,** 215–228.
34. Bueno, O. F., Wilkins, B. J., Tymitz, K. M., Glascock, B. J., Kimball, T. F., Lorenz, J. N. & Molkentin, J. D. (2002) *Proc. Natl. Acad. Sci. USA* **99,** 4586–4591.
35. Oie, E., Bjornerheim, R., Clausen, O. P. & Attramadal, H. (2000) *Am. J. Physiol.* **278,** H2115–H2123.
36. van Rooij, E., Doevendans, P. A., Crijns, H. J., Heeneman, S., Lips, D. J., van Bilsen, M., Williams, R. S., Olson, E. N., Bassel-Duby, R., Rothermel, B. A. & De Windt, L. J. (2004) *Circ. Res.* **94,** e18–e26.
37. Bueno, O. F., van Rooij, E., Molkentin, J. D., Doevendans, P. A. & De Windt, L. J. (2002) *Cardiovasc. Res.* **53,** 806–821.
38. Vega, R. B., Rothermel, B. A., Weinheimer, C. J., Kovacs, A., Naseem, R. H., Bassel-Duby, R., Williams, R. S. & Olson, E. N. (2003) *Proc. Natl. Acad. Sci. USA* **100,** 669–674.
39. Fiedler, B. & Wollert, K. C. (2004) *Cardiovasc. Res.* **63,** 450–457.
40. Li, H. H., Kedar, V., Zhang, C., McDonough, H., Arya, R., Wang, D. Z. & Patterson, C. (2004) *J. Clin. Invest.* **114,** 1058–1071.